A Study of Lubricating Flows in MEMS Bearings

J. Streeter[1] and E. Gutierrez-Miravete[*,2]
[1]Optiwind, [2]Department of Engineering and Science, Rensselaer at Hartford
*Corresponding author: 275 Windsor Street, Hartford, CT 06120, gutiee@rpi.edu

Abstract: The bearing and shaft are part of a safe and arm device constructed as an assembly by a multi-layer additive/subtractive plating and planarization processes (EFAB technology). Devices are constructed by a multi-layer additive/subtractive planarization process. This paper evaluates the lubricating flow between the shaft and journal of the MEMS bearing for seven configurations. The pressure differential was used to rank the designs.

Keywords: Bearings, Lubrication, Tribology, MEMS

1. Introduction

In the trend towards miniaturization, Microelectromechanical (MEMS) devices have been attracting a great deal of attention. An important issue affecting device performance is the tribological behavior of the various device components during operation. In this work the lubricating behavior of a MEMS bearing has been investigated using the CFD module in COMSOL Multiphysics. The bearing and shaft are part of a safe and arm device and are constructed as an assembly by microelectronic fabrication consisting of multi-layer additive/subtractive plating and planarization processes (EFAB technology) which can achieve sub micron resolution. The technique is flexible and facilitates creation of assembled multi-component devices.

Figure 1 shows a cross section of a typical bearing device considered. The two 0.1mm diameter shafts appear on the top and bottom. There is 0.006mm clearance between the thrust surface and the rotating element. The radial clearance of the shaft is 0.01 mm. In addition, there is 0.036 mm clearance between the edges of the rotating element and the bearing cage. When subjected to centrifugal loads, the rotating element moves an explosive charge from the safe to armed position.

Since various candidate bearing designs can be readily produced, it is important to be able to discriminate these in terms of their tribological performance. The goal of the study was to compare various proposed bearing designs in terms of the flow behavior of the lubricating fluid separating the bearing from the shaft. The evaluated designs are a standard journal, four-lobe and six-lobe configurations. For the lobed configurations, the voids are a channel, diffuser or nozzle.

Figure 1. Cross-section of a MEMS bearing

2. Use of COMSOL Multiphysics

During regular operation, the relative motion between the rotating shaft and the thrust surface produces flow in the intervening fluid (air). COMSOL Multiphysics was used to create two dimensional models of seven distinct MEMS bearing geometries and to compute the lubricating flow in each case. To simplify the problem, a small bearing offset was imposed to simulate the displacement due to applied load. In each case, the minimum clearance was maintained at 30 μm, the pressure was set to zero on the shaft and a rotational velocity of 4000 rpm was imposed on the shaft. The effect of shaft offset was evaluated for each of the seven configurations, and the pressure differential was calculated. The default mesh created by the software was used, together with one or two levels of automatic refinement. All calculations produced mesh independent results when using about 4000 elements.

3. Mathematical Formulation

Governing Equations: The mathematical formulation of the problem requires the statement of the continuity equation and the momentum balance (Navier-Stokes) equations for the air in the gap under steady state and laminar flow conditions, namely

$$\nabla \cdot \mathbf{U} = 0\,,$$

$$\rho \frac{\partial \mathbf{U}}{\partial t} = \rho \boldsymbol{g} - \nabla p + \mu \nabla^2 \mathbf{U}$$

Boundary Conditions:
The velocity on the surface of the shaft is set to the rotational velocity, 419 rad/s.

$u_{shaft} = -\omega x$

$v_{shaft} = -\omega y$

The pressure on the surface of the shaft is set to zero.

$P_{shaft} = 0$

The velocity normal to the surface of the bearing journal is set to zero, enforcing a no-slip condition.

$\overrightarrow{v_{journal}} = \vec{v} \cdot \widehat{n_{normal}} = 0$

For the flow field, the density and viscosity are set to standard atmospheric conditions for air.

$\rho_{air} = 1.225\ {}^{kg}/_{m^3}$

μ_{air} =0.0.000018 kg/m s

4. Results

A selected set of computed results is now presented. For all of the simulations, the clearance between the shaft and bearing was maintained at 30 µm.

Figure 2 shows the pressure and velocity obtained for the journal bearing due to shaft offset and rotation.

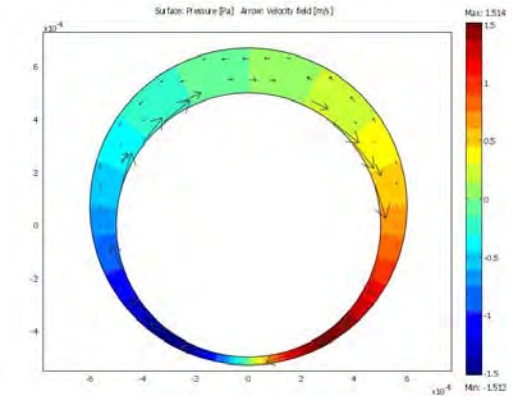

Figure 2. Journal Bearing with 0° Offset

An area of recirculation occurs on the top half of the bearing as evidenced by the small velocity vectors pointing opposite to the direction of shaft rotation. An identical pressure differential was calculated with the shaft offset at 30 and 45 degrees.

Figure 3 shows the computed results for a four lobbed bearing. Each channel of the bearing is 42 µm wide by 42 µm long. All of the channels show the formation of eddies. These vortices may account for the lower pressure differential achieved by this configuration. A high pressure region is seen in the left channel, while a low pressure region is seen in the right channel.

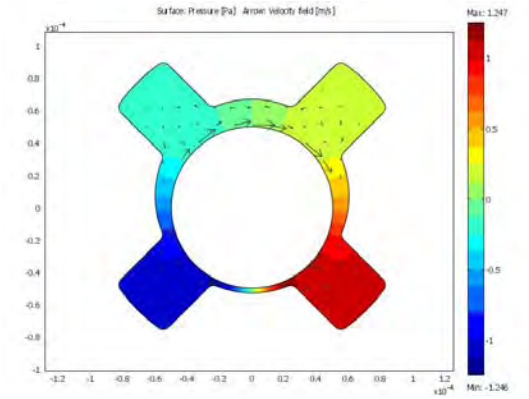

Figure 3. 4-Channel Bearing with 0° Offset

Results for the four-lobed diffuser are shown in Figure 4. This arrangement produced the lowest pressure differential of all the configurations. Each diffuser has an inlet width of 42 µm, a length of 40 µm and an angle of 30°. The high pressure region has migrated to the bottom of the bearing. A low pressure region can be seen at the left center. Vortices develop in each of the diffuser sections. The pressure differential is more than one Pascal less than the zero degree offset model.

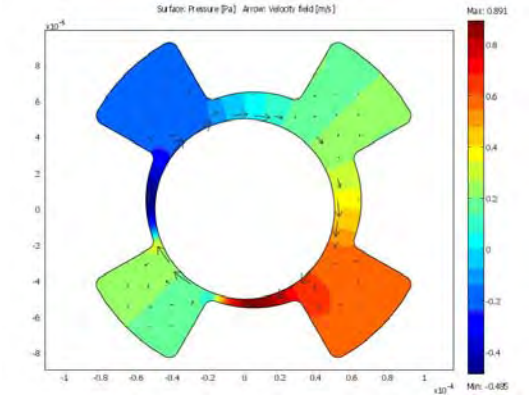

Figure 4. 4-Diffuser Bearing with 45° Offset

Figure 5 shows the computed results for the 6-nozzle bearing. Each of the six nozzles has an inlet width of 32 µm, a length of 42 µm and a taper angle of 20°. Eddies are formed in all of the nozzles. A high pressure area occurs in the lower right nozzle that causes the air to flow

towards the low pressure region in the lower left nozzle. The pressure differential is the highest of the lobed configurations.

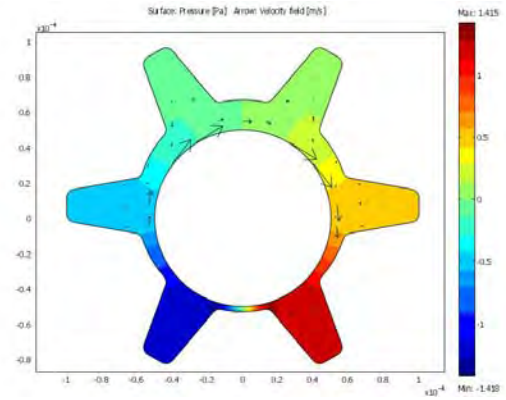

Figure 5. 6-Nozzle Bearing with 0° Offset

Table 1 summarizes the main findings of the study in terms of the computed pressure differential obtained. The 6-lobe diffuser produced the lowest value and the plain journal bearing the highest.

Configuration	Nominal	Offset
Journal	3.026	3.023
4-Lobe Channel	2.493	1.440
4-Lobe Nozzle	2.573	1.508
4-Lobe Diffuser	2.427	1.376
6-Lobe Channel	2.785	1.758
6-Lobe Nozzle	2.833	1.788
6- Lobe Diffuser	2.624	1.666

Table 1. Computed Pressure Differentials

5. Conclusions

The nozzle designs consistently produced the largest pressure differential among the lobed configurations. In addition, all the six lobe configurations exceed the results of the four lobe designs. When the shaft is directly above the channel, nozzle or diffuser, the highest pressure differential is still more than forty percent less than the journal bearing.

The best of the lobe designs contains six nozzle sections. It produces within 7% of the pressure differential of the journal bearing with zero degrees offset. However, with forty-five degrees offset, less than 60% of the journal differential is created.

6. References

1. Bhushan, B., Introduction to Tribology, John Wiley & Sons, New York (2002)